# Inversion of total and differential cross-section data for electron-methane scattering

D. R. Lun, K. Amos, and L. J. Allen
*School of Physics, University of Melbourne, Parkville, Victoria 3052, Australia*
(Received 27 April 1995; revised manuscript received 5 October 1995)

The inverse scattering theory has been used to define effective local electron-methane interaction potentials. Those interactions have been obtained first by inversion of the total cross-section data as a function of energy. The WKB approximation has been used in that determination. The same approximation has been used to effect (fixed energy) inversion of differential cross-section data from electron-methane scattering for energies of 200, 300, 500, and 700 eV. The resulting interactions, which we have assumed to be purely real, are very similar and show little energy dependence. They are in good agreement with a theoretically derived potential for this system at those radii for which the inversion potentials are determined sensitively by the scattering data. In addition, the generalized unitarity theorem has been used to specify the scattering amplitude from the 700-eV data. The $S$ function given by Legendre integration of that amplitude has been inverted to specify another purely real potential for the collision. The result is very similar to those found by the other analyses.

PACS number(s): 34.80.−i

## I. INTRODUCTION

There are two basic approaches with which quantitative information on the (effective local) interaction between two particles undergoing nonrelativisitic quantal scattering may be specified. The most common is the direct approach in which an interaction potential is obtained by making a ''first principles'' calculation based upon specifics of more fundamental underlying two particle interactions. The derived potential then is used in direct solution of the Schrödinger equation and the asymptotic properties of the relative motion wave functions give the predictions to be compared with measured data.

The alternative approach is to use inverse scattering theory [1], with a most common approach in this vein being that of numerical inversion. Therein one first makes an informed choice of a phenomenological form for the interaction and then, by adjusting the values of associated parameters, repeated solutions are made of the Schrödinger equations until a best fit is found to the data set of interest. But there are more rigorous inverse scattering theories [1] with which the (Schrödinger) interaction can be constructed directly from the scattering function. With these more rigorous methods, essentially no *a priori* assumption is made about the shapes of the potentials, although they will belong to the class identified with the specific method used. By dint of their construction, however, and when used in direct solutions of the Schrödinger equation, they give (retain) an extremely high quality fit to the data upon which they were predicated. They may or may not be ''realistic'' insofar as they do or do not look like ones determined by folding underlying elementary two particle interactions with the density profiles of many body colliding systems. If they do then one may take heart that the measured data are reflecting the inherent character of the many body theory considered. If they do not, that is no proof that the many body theory is wrong, but that many body theory must lead in finality to an interaction that provides a statistically significant fit to the data.

The interaction that results from inverse scattering theory usually is associated with an excellent fit to the data. That is by design and one should not assume that the potential found is physical. There are ambiguities in the process [1] and with the methods we will use in particular [2]. With the direct approach, in contrast, one is able to incorporate physical knowledge and insight at the outset. But direct analyses of scattering data often do not give a quality fit, as measured, for example, by the $\chi^2$ per datum ($\chi^2/N$) not being of order one [3]. The best situation is one in which a model interaction constructed from first principles and which gives a reasonable fit to the data is used to regularize the inversion process that yields a refined interaction with which an excellent fit to that data set results. But a prerequisite for such a procedure is an extraordinarily high quality data set so that variation of $\chi^2/N$ is a stringent selection criterion upon the model specifics.

Inversion methods usually belong to one of two classes, the first of which has energy as the spectral parameter and the angular momentum is fixed, the second is vice versa. Of the latter, the fixed energy class, we have found that the fully quantal and semiclassical WKB inversion schemes of Lipperheide-Fiedeldey (LF) type [4,5] have been most useful in practice. Those schemes have been used extensively in recent years to analyze the differential cross sections from the elastic scattering of two nuclei [5,6] as well as of electrons from water molecules [7] and from atoms [8]. In this paper, we analyze the differential cross-section data [9] for $e$-$CH_4$ scattering using the semiclassical WKB inversion scheme of LF type and construct local inversion potentials at energies ranging from 200 eV to 700 eV. Differential cross-section data at other, and lower, energies exist but we have chosen the set from Sakae *et al.* [9] as they are typical of a modern experiment, have been taken at energies for which the WKB method may be applicable, and were provided to us in tabular form with specified error values.

While most of the applications of inverse scattering theory take differential cross-section data as the starting point, Miller [10] has shown that it is also possible to obtain potentials by inversion of the total cross section. His method is based on an eikonal approximation and on the assumption that the potential is real, local, and independent of energy

 

(i.e., there is no underlying nonlocality). It has been used [11] to specify an interaction for the He-He atomic system. Herein we demonstrate that the approach can be used also with a WKB approximation as the Sabatier transform [1] links the (inversion) potential to the quasipotential which is defined by the phase shift function associated with the scattering. The Miller procedure [10] can be used equally well to specify that quasipotential. The assumption that the quasipotential is independent of energy facilitates the scheme, but, by virtue of the Sabatier transform, there is a residual energy dependence in the extracted interaction. We present this development herein since many total cross-section measurements have been made for the scattering of electrons from atoms and molecules. In some cases those measurements span a wide energy range. For example, recent measurements at incident electron energies of up to 4 keV have been reported [12]. We are not aware of any previous inversion analyses of the total cross sections for electron scattering and here we investigate the feasibility of such and compare inversion potentials calculated from total cross-section data with one obtained by direct calculation, as well as with ones found using fixed energy inversion of a select set of differential cross sections.

At low energies, $\leqslant 60$ eV typically, *ab initio* calculations of effective interactions for electrons scattering from small molecules have shown that static, exchange, and polarization (SEP) components are all important in an explanation of the total elastic scattering cross sections [13] and that has also been observed specifically for the case of methane [14,15]. In a later publication, Jain [16] used a complex optical potential which, for energies above 20 eV, had an energy dependent absorptive part that significantly reduced calculated elastic scattering (total) cross sections. His static exchange, asymptotically adjusted polarization plus absorption model calculations have strong absorption in the energy regime 100 – 500 eV, an energy region of interest to us. He also predicted differential cross sections at 100, 200, 300, and 400 eV with those complex potentials. Data were not available then for all of those energies, but the 200-eV measurement had been made. In a previous paper [14], those 200-eV differential cross-section data were analyzed and reasonably well fitted by a calculation in which only a purely real (SEP) potential was used. The prediction with the absorptive interaction of Jain [16] does not fit nearly as well. But a refined complex interaction could well do so. The question is just how absorptive that interaction would (or should) be. This and the data of Sakae *et al.* [9] at many energies to 700 eV, together with our ability to use inversion of the total and differential cross-section information, motivated our present report. In particular, we have analyzed the total cross-section data from electrons scattered from methane molecules, and have considered the relevant differential cross-section data [9] for the elastic scattering of 200-, 300-, 500-, and 700-eV electrons.

Herein we have restricted consideration to finding purely real interactions. The methods (of inversion) used need not be so restricted. They can be used to specify complex (absorptive) interactions. But by restricting consideration to real interactions, the number of parameters involved in the first stage of inversion, namely, the determination of an $S$ function form from an excellent fit to the data, is reduced markedly. The results are much less ambiguous then and demonstrate that, if absorptive processes are important in the reaction mechanism, these scattering data should not be used solely as the measure of those contributions. By considering purely real interactions, the $S$ function is unitary and the generalized unitarity theorem permits one to determine the actual scattering amplitude $f(\theta)$ from the scattering data. The magnitude of $f(\theta)$ is the square root of the differential cross section and its phase is a solution of a nonlinear integral equation [the kernel of which involves the complete $(0°–180°)$ cross section] [17]. If a stable solution of that nonlinear equation can be found [18,19] then the $S$ function is given exactly by Legendre integrations of the (complex) scattering amplitude. The starting ''data'' for the inversion methods is then fixed with little ambiguity and so poses a stringent constraint on the specifics of the $S$ function form to be used in subsequent inverse scattering calculations.

The inversion procedures that we have used are presented in Sec. II as is a brief review of the process of using the generalized unitarity theorem to define scattering phase shifts. The results of our applications to the analyses of electron scattering from the molecule $CH_4$ are then presented and discussed in Sec. III. Conclusions we can draw are given finally in Sec. IV.

## II. INVERSION THEORY AND METHODS

Direct and inverse methods of analysis of scattering data usually are processes that involve two stages, with the link between the measured data and the interaction potential being the scattering matrices $S_\ell(k)$ or equivalently, the scattering phase shifts $\delta_\ell(k)(=(1/2i)\ln[S_\ell(k)])$. For the scattering of spinless particles, or if the intrinsic spin of the projectile is ignored (as is the case here), only real half-integer values of the angular momentum variable $\lambda$ (i.e., $\lambda=\ell+1/2$) are required and the differential cross sections at a fixed energy and with scattering angle $\theta$ are given in terms of (complex) scattering amplitudes,

$$f(\theta)=\frac{1}{k}A(\theta)e^{i\varphi(\theta)} \tag{1}$$

by

$$\frac{d\sigma(\theta)}{d\Omega}=|f(\theta)|^2=\frac{1}{k^2}A^2(\theta)$$

$$=\frac{1}{4k^2}\left|\sum_{\ell=0}^{\infty}(2\ell+1)[S_\ell(k)-1]P_\ell(\theta)\right|^2, \tag{2}$$

while the total cross section for scattering by a purely real interaction is given by

$$\sigma(k)=\frac{4\pi}{k^2}\sum_{\ell=0}^{\infty}(2\ell+1)\sin^2[\delta_\ell(k)]. \tag{3}$$

Therein the phase shifts are purely real quantities as absorptive processes have not been considered. The wave numbers are defined from the center of mass energy as usual by $E=(\hbar^2/2\mu)k^2$. Then, if the phase shifts $\delta_\ell(k)$ can be inter-

polated smoothly, the infinite summation in Eq. (3) can be converted to an integral so that the total cross section becomes

$$\sigma(k)=\frac{4\pi}{k^2}\int_0^\infty 2\lambda\sin^2[\delta(\lambda,k)]d\lambda, \tag{4}$$

where $\delta(\lambda,k)$ is a continuous function of $\lambda$.

With scattering by real potentials, the magnitude and phase of the amplitudes [Eq. (1)] may be extracted from the measured differential cross sections, under the constraint that the scattering function is unitary [17]. In such cases the generalized unitarity theorem leads to an equation defining the phase $\varphi(\theta)$ in terms of the complete (0°–180°) cross section, viz., with $x=\cos(\theta)$,

$$\sin\varphi(x)=\int\int\frac{A(y)A(z)\cos[\varphi(y)-\varphi(z)]dy\ dz}{2\pi A(x)(1-x^2-y^2-z^2+2xyz)^{1/2}}. \tag{5}$$

Therein the region of integration is the interior of an ellipse. From the specified (complex) scattering amplitude, the scattering function is obtained by

$$S_\ell-1=e^{2i\delta_\ell}-1=ik\int_0^\pi f(\theta)P_\ell(\theta)\sin(\theta)d\theta, \tag{6}$$

which in turn identifies the phase shifts $\delta_\ell$.

Usually, solutions of Eq. (5), or its equivalent, have been sought with iteration schemes based on the contraction mapping principle [17,18]. That approach also defines an existence condition for a solution and for its global uniqueness as well. In application, though, we have found difficulties with it. The physical circumstances considered [19] did not meet the domain criteria and the solutions found were not stable. Thus we considered a modification of the Newton iteration method.

In brief, our modified Newton method [19] considers an operator $F$ acting on functions $\varphi$ according to

$$F[\varphi]=\sin[\varphi(x)]-\int\int\frac{A(y)A(z)\cos[\varphi(y)-\varphi(z)]dy\ dz}{2\pi A(x)(1-x^2-y^2-z^2+2xyz)^{1/2}}. \tag{7}$$

The Fréchet derivative $F'$ of $F$ is given by

$$\begin{aligned}F'_\varphi(h)&=\cos[\varphi(x)]h(x)+\int\int H(x,y,z)\sin[\varphi(y)-\varphi(z)]\\&\quad\times[h(y)-h(z)]dydz\\&=\cos[\varphi(x)]h(x)+2\int\left(\int H(x,y,z)\sin[\varphi(y)\right.\\&\quad\left.-\varphi(z)]dz\right)h(y)dy\end{aligned} \tag{8}$$

and is a bounded linear operator. Then, if one can solve the linear functional equation,

$$F(\varphi^n)+F'_{\varphi^n}(\varphi^{n+1}-\varphi^n)=0, \tag{9}$$

for $\varphi^{(n+1)}$, and if the sequence $\varphi^n$ converges, its limit is a solution of Eq. (5). Further, if the integral in Eq. (8) is approximated by a quadrature formula, Eq. (9) reduces to a system of linear equations. However, the price of finding stable convergent solutions by this means is the loss of a rigorous guarantee of global uniqueness.

We now describe the two methods of inversion of actual data; the first associated with the total cross-section data and the second of fixed energy form appropriate for the differential cross-section data. Both use the WKB approximation to facilitate a link between measurement (phase shifts) and an interaction (Schrödinger) potential.

In the WKB approximation [1,5], the phase shift function relates to a quasipotential $Q(\sigma)$ by

$$\delta(\lambda,k)=-\frac{\mu}{\hbar^2k^2}\int_\lambda^\infty\frac{Q(\sigma)}{\sqrt{\sigma^2-\lambda^2}}\sigma d\sigma, \tag{10}$$

which, by an Abel integral transform [1], gives the quasipotential as

$$Q(\sigma)=\frac{4E}{\pi}\frac{1}{\sigma}\frac{d}{d\sigma}\left(\int_\sigma^\infty\frac{\delta(\lambda,k)}{\sqrt{\lambda^2-\sigma^2}}\lambda d\lambda\right). \tag{11}$$

The scattering potential then is specified by the Sabatier transform,

$$V(\rho)=E\left[1-\exp\left(-\frac{Q(\sigma)}{E}\right)\right], \tag{12}$$

so long as there is a 1 to 1 correspondence between $\rho$ and the dimensionless variable $\sigma$ via the transcendental equation

$$\rho=kr=\sigma\ \exp\left(\frac{Q(\sigma)}{2E}\right). \tag{13}$$

### A. Inversion of total cross sections

With $\sigma=ks$, one can rewrite the WKB approximation for the phase shift function, Eq. (10), in terms of an impact parameter, $b(=\lambda/k)$, viz.,

$$\delta(\lambda,k)=-\frac{\mu}{\hbar^2k}\int_b^\infty\frac{Q(ks)}{\sqrt{s^2-b^2}}sds\equiv\frac{1}{2k}\omega(b). \tag{14}$$

Miller [10] assumed $Q(ks)$ to be independent of the momentum $k$ so that $\omega(b)$ is also. Then if $\omega(b)$ is a smooth, invertible function, an Abel inversion of Eq. (14) yields

$$Q(ks)\to Q(s)=-\frac{\hbar^2}{\pi\mu}\int_0\frac{1}{\sqrt{b^2(\omega)-s^2}}d\omega. \tag{15}$$

The upper limit of the integral is the value for which the radicand is zero. Miller assumed further that the quasipotential was small so that a first order expansion of the transcendental equations equates the potential to the quasipotential directly with $s\to r$. Then Eq. (15) reduces to that used by Miller and defining the potential $V_M(r)$, viz.,

$$V_M(r) = -\frac{\hbar^2}{\pi\mu}\int_0 \frac{1}{\sqrt{b^2(\omega)-r^2}}\,d\omega. \tag{16}$$

The latter approximation of Miller is not essential. The method he set forth can be used to obtain the quasipotential itself and the Sabatier transform then gives the interaction potential.

To obtain $b(\omega)$ from the total cross section, one may proceed by integrating (by parts) the integral equation for the total cross section, Eq. (4), to get

$$\sigma(k) = \frac{4\pi}{k^2}[\lambda^2 \sin^2\{\delta(\lambda,k)\}]_0^\infty$$

$$-\frac{4\pi}{k^2}\int_0^\infty \lambda^2 \sin\{2\delta(\lambda,k)\}\left(\frac{d\delta(\lambda,k)}{d\lambda}\right)d\lambda. \tag{17}$$

For potentials decreasing faster than $r^{-3}$ as $r\to\infty$, the phase shifts decrease faster than $\lambda^{-2}$ as $\lambda\to\infty$ [4], and therefore the leading term in Eq. (17) vanishes. A change of variables then gives

$$k\sigma(k) = 2\pi\int_0^\infty b^2(\omega)\sin\left(\frac{\omega}{k}\right)d\omega, \tag{18}$$

whose Fourier sine transformation,

$$b^2(\omega) = \frac{2}{\pi^2}\int_0^\infty \sigma(k)\sin\left(\frac{\omega}{k}\right)k\,dk, \tag{19}$$

is a direct specification of $b^2(\omega)$ in terms of the total cross-section data. But it is not very practical as there are numerical difficulties with integration when $\omega$ is large, and the measured data are usually far from complete functions of $k$. Thus we propose to use a functional form for $b^2(\omega)$ in Eq. (18) to fit measured total cross-section data. Specifically we have chosen the form

$$b^2(\omega) = \frac{A}{\omega(B^2+\omega^2)^2}, \tag{20}$$

with the parameters $\{A,B\}$ to be determined by a $\chi^2$ minimization search giving a ''best fit'' to the measured data. It is of note that the cross section with this form for $b^2(\omega)$ has the asymptotic form

$$\sigma(k) = \frac{\pi^2 A}{B^4 k}\left\{1-\left(1+\frac{B}{2k}\right)\exp\left(-\frac{B}{k}\right)\right\}$$

$$\to \frac{\pi^2 A}{2B^3k^2} + \mathcal{O}(k^{-4}) \quad \text{as} \quad k\to\infty. \tag{21}$$

With this selected form for $b^2(\omega)$ the quasipotential $Q(s)$ as a function of $s$ is easily obtained from Eq. (15). The inversion potential as a function of $r$ is then found by use of the transcendental equations, Eqs. (12) and (13), for each energy, and is designated hereafter as $V_Q(r,E)$.

### B. Fixed energy inversion of differential cross sections

Since the foregoing discussion of inversion of total scattering cross-section data involves the (complete) phase shift function, we can define the fixed energy phase shift function $\delta(\lambda,k)$ at any single energy for use with a (fixed energy) WKB inversion scheme. Alternatively we can take each differential cross section as a separate data set to be used in a fixed energy inversion scheme by first defining an $S$ function of the appropriate form from its direct fit to the (fixed energy) data. With both approaches, we consider the WKB method that we have used in the past [5–8] to analyze other differential cross-section data. Consequently we give herein but a brief review of the fixed energy method to define terms to be used in the later discussion.

This approach is based upon using known forms for the phase shift function for a fixed energy, within the Abel integral transform, Eq. (11), to specify the (fixed energy) quasipotential. The inversion potential, at the chosen energy, is given then by the Sabatier transform, Eq. (12), and at radii specified by the relation Eq. (13). Potentials calculated in this way will vary with the chosen energy, but as they are determined by using a fixed energy inverse scattering method, we identify them hereafter as $V_{\rm FE}(r,E)$. To apply the fixed energy inversion scheme, it is particularly useful to recast the (fixed energy) phase shift function in the form

$$\delta(\lambda,k) = \frac{1}{2i}\sum_{n=1}^{N}[\ln\{\lambda^2-\alpha_n^{*2}\}-\ln\{\lambda^2-\alpha_n^2\}], \tag{22}$$

for which the $S$ function has the rational form

$$S(\lambda,k) = \prod_{n=1}^{N}\left(\frac{\lambda^2-\alpha_n^{*2}}{\lambda^2-\alpha_n^2}\right), \tag{23}$$

as then the quasipotential is given explicitly by

$$Q(\sigma) = 2iE\sum_{n=1}^{N}\left[\frac{1}{\sqrt{\sigma^2-\alpha_n^2}}-\frac{1}{\sqrt{\sigma^2-\alpha_n^{*2}}}\right]. \tag{24}$$

This form has been used with success in WKB inversion studies of nuclear, atomic, and molecular scattering (differential) cross sections [6–8] and we now apply it by finding the optimal smallest set of complex (conjugate) pole-zero pairs by a direct fit to the actual measured differential cross section. A least squares search has led to sets of (two) values $\{\alpha_n\}$, that give excellent fits to the differential cross-section data [9] taken at 200, 300, 500, and 700 eV. Those values are listed in Table I along with the $\chi^2/F$ for each fit. Again as we have restricted the pole-zero pairs to be complex conjugates, each energy inversion will yield a purely real interaction.

## III. RESULTS AND DISCUSSION

### A. Inversion of the total cross-section data

The procedures to invert total cross-section data have been used to determine inversion potentials for the interactions of electrons with the $CH_4$ molecules [12]. Total cross-section data for all have been taken in the range from 77.5 eV up to 4 keV, a spread which makes feasible use of the inversion method. The data were fit using the parametric

TABLE I. The two complex poles $\alpha_n$ defining the scattering functions obtained from fits to the differential cross sections for electron elastic scattering from $CH_4$. The zeros, $\beta_n$, are the complex conjugates of these. The quality of the fits is specified by the values of the $\chi^2/F$ that are shown in the second column.

| Energy (eV) | $\chi^2/F$ | $\alpha_1$ | $\alpha_2$ |
|---|---|---|---|
| 200 | 1.00 | (1.368, 3.605) | (0.8918, 0.6875) |
| 300 | 0.54 | (1.211, 4.231) | (0.9481, 0.8322) |
| 500 | 0.63 | (1.757, 3.758) | (0.5971, 0.7887) |
| 700 | 0.88 | (1.728, 3.766) | (0.5288, 0.8003) |

form for $b^2(\omega)$ given by Eq. (20) and the optimal values of the parameters are $8.462\times10^5$ and 19.96 for $A$ and $B$, respectively. With those parameter values, the quality of the fit to the data is measured by the value of $\chi^2/F$ being 1.7. Inverting the $b^2(\omega)$ functions gives phase shift functions per Eq. (14), and to check that quality fits to the data have been retained by the assumed energy dependence, those phase shift functions were used in the partial wave summations of Eq. (3) to compare with the data a second time. The $\chi^2/F$ after that process is 1.9. Clearly the adopted form for the phase shift function retains the quality of fit to data quite well and the integral formula, Eq. (4), is therefore a reliable approximation with this data set.

The fits to the total cross-section data that are shown in the top segment of Fig. 1 are the results of recalculations using the inversion potentials $V_Q(r,E)$ in the Schrödinger equation. These recalculated total cross sections are also very similar to ones found using the Miller inversion potentials $V_M(r)$ as is evident from the energy variation of the difference,

$$\Delta(k)=100\left[\frac{\sigma_Q(k)-\sigma_M(k)}{\sigma_Q(k)}\right], \tag{25}$$

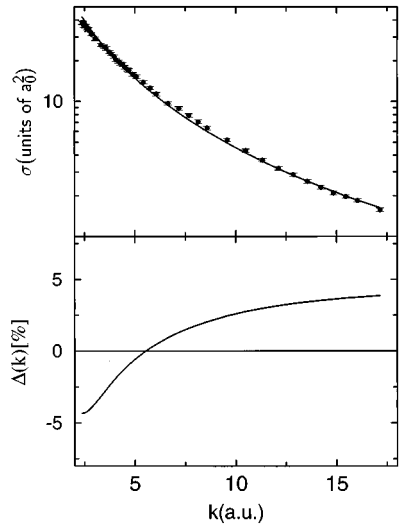


FIG. 1. The total cross-section data from electron scattering from the $CH_4$ molecule are compared in the top section with the results calculated by using the inversion potentials $V_Q(r,E)$. In the bottom section, the percentage difference $\Delta(k)$ between total cross sections calculated using our WKB prescription and the Miller one are displayed.

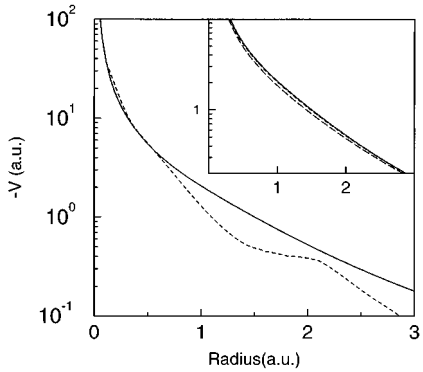


FIG. 2. The potential (solid curve) $V_Q(r,1000$ eV) from the inversion of the total cross section from $e$-$CH_4$ scattering compared with the result of a model calculation (dashed line) [14]. The insertion shows the inversion potentials $V_Q(r,E)$ obtained at 1000 eV (solid line), 400 eV (small dashed line), and 100 eV (long dashed line), respectively.

that is plotted in the bottom segment of Fig. 1. Here $\sigma_Q(k)$ and $\sigma_M(k)$ are the total cross sections found using the inversion potentials given by our WKB scheme and with Miller's eikonal approximation, respectively. Evidently for most energies ($k>5$ Å$^{-1}$) the difference is but a few percent.

The potentials from our analyses of the $e$-$CH_4$ total cross-section data are shown in Fig. 2. In the main feature of this diagram, the inversion potential $V_Q(r,1000$ eV) is displayed by the solid curve. We chose that energy to be large enough that the WKB approximation is valid and that the quasipotential values would be small so that the Miller prescription should be valid. Indeed the resultant inversion potential is virtually identical to $V_M(r)$ obtained using the Miller prescription. The inversion result is compared also with the result of a theoretical calculation (displayed by the dashed curve) and which is a sum of static, polarization, and exchange potentials for the $e$-$CH_4$ system [14]. The inversion potential is larger than the model calculation at radii greater than 0.8 a.u. The results of our WKB calculations of $V_Q(r,E)$ for $e$-$CH_4$ scattering at different energies are shown in the inset. There is practically no difference between the 400- and 1000-eV results (short dashed and solid curves, respectively) so that the Miller assumption that the underlying potential is energy independent is met, at least for this energy regime. Further, the agreement of these results with $V_M(r)$ indicates also that the eikonal approximation is very good at energies above 400 eV. The 100-eV result in the inset is shown by the long dashed curve. It does differ slightly from the other two and, while we may expect such as a breakdown of the high energy approximations of our inversion studies, it can also be a reflection that absorptive processes, ionization, in particular, are now more important as well. In a mean field theory such are accounted for by having complex, optical potentials.

But the (total cross section) inversion method is most accurate for small $r$ values [10]. By recalculating the total cross sections with the inversion potentials altered to have $r^{-4}$ form at radii greater than a value $R_{\rm cut}$, we found that the energy variation (of the total cross section) was little altered. The absolute magnitudes were with 10% and 20% reduction occurring for $R_{\rm cut}$ being 3.0 and 2.0 a.u., respectively. There-

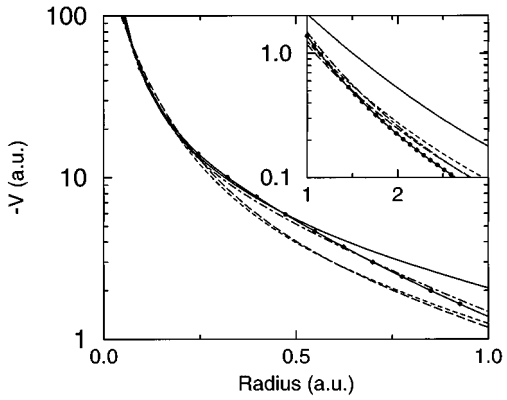


FIG. 3. The potentials determined by fixed energy inversion of the differential cross-section data [9] and displayed by the dashed, long dashed, dot-dashed, and chain line for the 200-, 300-, 500-, and 700-eV cases, respectively, compared with the $V_Q(r,1000\ \text{eV})$ found from inversion of the total cross section (solid line).

fore the large radii aspect of the potential is not established by the inversion study of the total cross-section data. So we consider next whether or not specific differential cross sections may be. In particular, we consider fixed energy inversion methods for data at energies where we are confident that the WKB approximation is valid.

### B. WKB fixed energy inversion of differential cross sections

We have used the fixed energy WKB inversion method to analyze the differential cross sections of $e$-$CH_4$ scattering at 200, 300, 500, and 700 eV [9]. Using the complex-conjugate pair values given in Table I to define the $S$ function at each energy gives quality fits to the data. Those pole-zero pair values then were used to specify the fixed energy inversion potentials $V_{\text{FE}}(r,E)$ that are shown in Fig. 3. Clearly, there is some energy dependence to these results, although for small radii ($r<1.0$ a.u.), they are all very similar to the $V_Q(r,1000\ \text{eV})$ result (shown by the solid curve in this figure) obtained by inversion of the total cross-section data. They differ from that and each other at larger radii though as is shown in the main body of the diagram for radii to 1 a.u. and in the inset for radii to 3.0 a.u. Using those fixed energy inversion potentials in the Schrödinger equation leads to the results that are shown in Fig. 3. Therein the data are compared with the calculated 200-, 300-, 500-, and 700-eV cross sections ranging from the top of the diagram to the bottom. Those cross sections have been scaled up by factors of 50, 10, 5, and 1, respectively, to facilitate viewing. Clearly the quality of fit is retained when the inversion potentials are used to recalculate the cross sections. The exact specification of the potentials beyond $\sim$ 2 a.u. does not influence these calculated cross sections very much, at least for the range of momentum transfer values spanned by the current data sets.

It is these results that set the standard by which the specific results found using our other calculations are to be measured. There are differences between the potentials found by inversion of the total cross section and those found from the fixed energy analyses. Those effects are considered next.

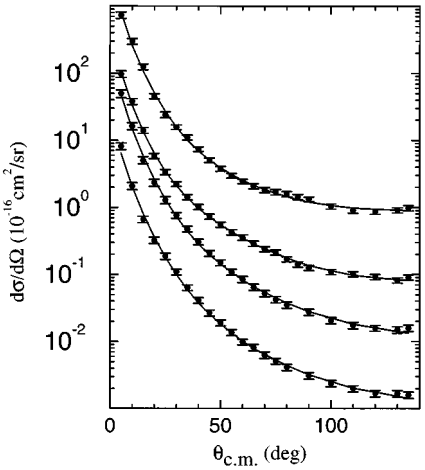


FIG. 4. The differential cross-section data at 200, 300, 500, and 700 eV (from top to bottom) compared with the results of using the fixed energy inversion potentials to recalculate them. The results have been scaled by 50, 10, 5, and 1 for the 200-, 300-, 500-, and 700-eV sets, respectively, to facilitate viewing.

### C. A comparison of the differential cross sections

The fixed energy (real) inversion potentials when used in the Schrödinger equation yield differential cross sections that are shown in Fig. 4. These calculations match the 200- to 700-eV data so well that we use the actual data as the equivalent of them to investigate the quality of the potentials obtained by inversion of the total cross-section data. We have made direct solution of the Schrödinger equations using $V_Q(r,200\ \text{eV})$ and $V_Q(r,700\ \text{eV})$ specifically to calculate the 200-eV and 700-eV differential cross sections. The comparisons of those cross sections with experimental data (and therefore with the fixed energy studies) are displayed in Fig. 5. The 700-eV results are given in the top panel and the 200-eV results are shown in the bottom. Therein the solid curves display the cross sections calculated using the $V_Q(r,E)$ interactions. The cross sections found by using theoretically derived interactions are also shown in Fig. 5. The (small) dashed curves represent the results tabulated by Jain [16] at 200 eV and calculated (at 700 eV) using the derived purely real interaction given in Ref. [14]. In the 200-eV case we show a third result (long dashed curve) which is the cross section obtained with a complex potential that has been proposed for this scattering [16]. Clearly the results at 700 eV are in quite good agreement with each other and the data. Thus at 700 eV the SEP model and the potentials from either fixed energy or total cross-section inversions are reasonably in agreement. They give very good to excellent fits to the measured differential cross sections with no need to include effects of absorption processes. Indeed, by changing the radial variation of $V_Q(r,700\ \text{eV})$ to have the expected polarization form at large radii reduces the calculated results at forward angles (essentially at 5° and 10° only) to agree with the data.

The 200-eV differential cross-section results are quite different, however. By its construction, the fixed energy potential gives an excellent fit to the data as was shown in Fig. 4, but of the set displayed in the bottom half of Fig. 5, the complex potential result (tabulated values in Ref. [16]) is very poor. That result is not in contradiction to the observed

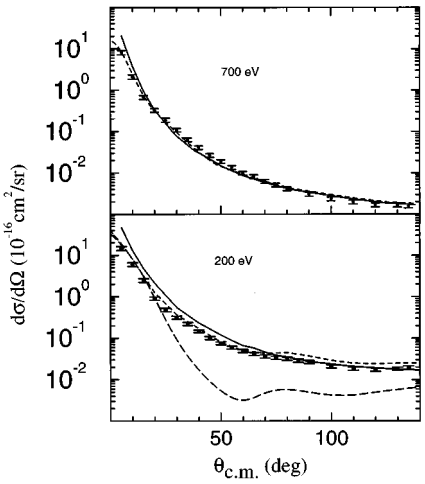


FIG. 5. The differential cross sections for $e$-$CH_4$ at 200 eV (bottom) and 700 eV (top). The solid curves are the results corresponding to the $V_Q(r,E)$ potentials while the (small) dashed curves are those found using a theoretical potential [14]. The long dashed curve at 700 eV is the cross section that results when a complex interaction [16] is assumed for this system.

reasonable result for the total cross section found in Jain's study since the misfit to the differential cross section occurs for data with magnitudes less than a few percent of the forward angle values. But the purely real (SEP) interaction result (also from the tabulation of Jain [16]) does very well for all angles to about 60° and then is only slightly larger than the remaining, small magnitude cross-section values. The result found using our $V_Q(r,200\ \text{eV})$ interaction overestimates the data at forward scattering angles but has the correct trend with momentum transfer. The good agreement at the higher momentum transfer (larger scattering angles) found using the $V_Q$ interaction is consistent with the total cross-section inversion method being more accurate for small radii than large. We varied the long range character of $V_Q(r,200\ \text{eV})$ to have the expected $r^{-4}$ form (from 1.5 a.u.) and again found changes in the forward angle cross-section prediction to bring agreement with the data. But that only affected the first two points (at 5° and 10°) seriously. The rest of the calculated cross section remained at odds with the measured values. At this energy then, only from fixed energy inversion have we a potential that we can tag with a quality fit to observed data.

### D. Use of unitarity to fix the $S$ function for inversion

The potentials found for 700-eV electron scattering are very similar and the fixed energy inversion analysis gives an excellent fit to the differential cross section. That process started with a search for a set of pole-zero complex-conjugate pairs of parameters to define an $S$ function from a ''best fit'' to the cross-section data. The process has ambiguities. But with unitarity as a constraint we can specify the physical $S$ function values directly from the data prior to inversion. The $S$ function parameters are then given by a simple mapping of the functional form to a table of numbers.

The data have been measured at scattering angles between 5° and 135°. To use the unitarity constraint that cross section is needed at all scattering angles. An interpolation has been made to obtain that complete cross section with the theoretical calculated values of Sakae *et al.* [9] at 0°, 160°, and 180° being used to facilitate that interpolation. With this input and initially the phase function taken to be the constant, $\varphi_0(\theta)=\varphi(0°)=0.287$, iteration of the nonlinear integral equation, Eq. (5), using our modified Newton method converged. The optical theorem gave the choice for $\varphi(0°)$.

TABLE II. The phase shifts (in degrees) obtained from the analysis of 700-eV electron–methane-molecule scattering data by unitarity condition, ($\delta_\ell^{(U)}$), compared with those of the rational $S$ function, ($\delta_\ell^{(S)}$), found by a direct fit of the differential cross section.

| $\ell$ | 0 | 1 | 2 | 3 | 4 | 5 | 6 |
|---|---|---|---|---|---|---|---|
| $\delta_\ell^{(U)}$ | 99.8 | 59.0 | 46.4 | 29.9 | 22.5 | 16.9 | 14.0 |
| $\delta_\ell^{(S)}$ | 102.9 | 62.0 | 44.0 | 32.9 | 24.8 | 19.0 | 14.8 |
| | 7 | 8 | 9 | 10 | 11 | 12 | 13 |
| $\delta_\ell^{(U)}$ | 11.6 | 9.8 | 8.0 | 6.5 | 5.1 | 4.2 | 3.5 |
| $\delta_\ell^{(S)}$ | 11.8 | 9.5 | 7.8 | 6.6 | 5.6 | 4.8 | 4.1 |
| | 14 | 15 | 16 | 17 | 18 | 19 | 20 |
| $\delta_\ell^{(U)}$ | 3.1 | 2.9 | 2.6 | 2.2 | 1.7 | 1.2 | 0.6 |
| $\delta_\ell^{(S)}$ | 3.6 | 3.2 | 2.8 | 2.5 | 2.3 | 2.0 | 1.8 |

The 20 phase shifts that could be calculated reliably by Legendre integration of the scattering amplitude found from the unitarity condition are given in Table II. They are compared with the set obtained from the $S$ function found by a direct fit to the cross-section data, i.e., with the pole-zero pair values given in Table I. The sets of phase shifts are quite similar, with differences in the important (low $\ell$) values being but a few percent. It is not surprising therefore that the $S$ function found by a simple mapping of the unitarity condition phase shifts is also very similar to the fitted one. With the phase shifts ($\delta_\ell^{(U)}$ up to $\ell=20$), we recalculated the differential cross section and the comparison with the experimental data and the (complete) shape that was input to the unitarity study are displayed in Fig. 6. Therein the solid curve is the input complete cross section and the dashed curve is the recalculation. Both are excellent fits to the data with the slight oscillatory behavior in the recalculation at large angles reflecting the truncation of the partial wave summation. The potentials that result from inversion in these cases are displayed in Fig. 7. The inversion potential based upon the unitarity condition results is displayed therein by the solid curve while the dashed curve is the fixed energy inversion one previously given in Fig. 3. The two differ slightly at small radii but are very similar from 0.3 a.u. outwards.

## IV. CONCLUSION

Purely real scattering potentials have been constructed by using inverse scattering theory to analyze both the total and a set of differential cross sections from the elastic scattering of electrons from $CH_4$. For energies above 200 eV, the inversion potentials show some energy dependence and those obtained by fixed energy inversion are associated with ex-

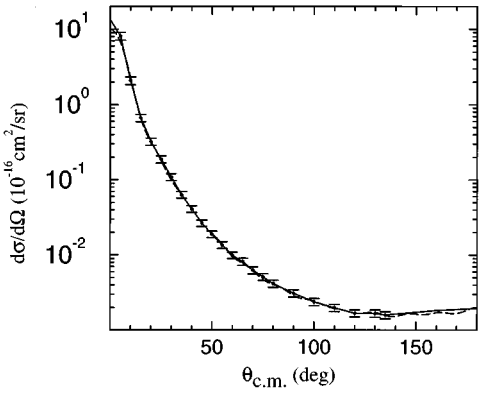


FIG. 6. The measured differential cross-section data and the interpolation and extrapolation of it (solid curve) from the elastic scattering of 700-eV $e$-$CH_4$ compared with the result (dashed curve) from the phase shifts which were found by using the modified Newton method to specify the scattering amplitudes.

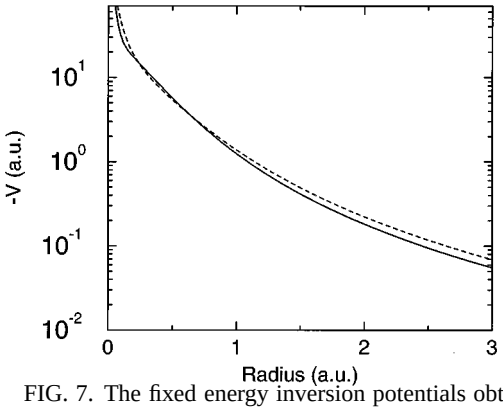


FIG. 7. The fixed energy inversion potentials obtained from the unitarity condition phase shift set (solid curve) and that from the $S$ function given by a direct fit to the cross-section data (dashed curve).

tremely good fits to the measured differential cross-section data. Likewise the potentials obtained by inversion of the total cross-section data reproduce those data quite well, but when used to analyze the 200- to 700-eV differential cross sections do not give the same quality of fits as the fixed energy inversion scheme. The large radii character of the total cross section (inversion) potentials is not correct.

The closely equivalent result for 700 eV based upon the phase shifts extracted using the unitarity condition confirm that there is little ambiguity for us to be concerned about with the search process that specifies the $S$ functions central to the fixed energy inversion process. The inversion schemes can be adapted to specify complex absorptive interactions but with the present data extremely good fits (to the 200- to 700-eV cross sections) did not require explicit inclusion of absorption effects. Other data, or more and very precisely measured differential cross-section data, will be needed to resolve just how strong absorption processes are in this scattering system. In particular, lower energy scattering data may be more instructive about absorption processes. Fully quantal inversion methods will be needed with those studies though.

The potentials obtained from inversion of the differential cross-section data are similar to the theoretical ones to radii $\sim 2$ a.u., and the results we have obtained suggest that the present data are rather insensitive to the precise values of the interaction at larger radii than this. That is not to say the system at lower energies or for smaller scattering angles (than 5°) will not be. Indeed, the cross sections of slow electron ($\leqslant 20$ eV) scattering are sensitive to the long range character of electron-molecule interactions. We also note that the inversion potentials are quite different from a (complex) interaction that has been proposed for this system. However, that may be of little significance since the fit to the differential cross-section data at 200 eV found by using that absorptive interaction is not good. Again, more data at smaller (and larger) momentum transfer values are needed if (differential) cross sections are to be sufficiently sensitive to the asymptotic properties of the interactions.

Inversion and direct studies of such scattering data are in fact complementary. With inversion studies, one can usually identify a potential that is associated with an excellent fit to data. But a fully microscopic folding model (direct) calculation is the only way to find the physical phenomena underlying any effective local interaction. Thus, given that a reasonable fit to data can be obtained with a microscopic direct calculation, by using that as a regularization inversion analyses then may indicate what attributes of the effective local interaction need be explained by even better microscopic model calculations. But high quality and extensive data sets are needed and, in the present case particularly, more data at both very small and large scattering angles are needed before such a regularization can be attempted with some hope for significant results.

## ACKNOWLEDGMENTS

We thank Dr. Takeji Sakae for providing us with tabulations of the differential cross-section data from the elastic scattering of electrons from $CH_4$.

[1] K. Chadan and P. C. Sabatier, *Inverse Problems in Quantum Scattering Theory*, 2nd ed. (Springer, Berlin, 1989).

[2] C. Steward, H. Fiedeldey, K. Amos, and L.J. Allen, Phys. Rev. C **51**, 836 (1995).

[3] A more appropriate quantity when parameter variations are involved in data analyses is $\chi^2$ per degree of freedom, $\chi^2/F$, where the degree of freedom is the number of data values $N$ less the number of parameters being varied.

[4] R. Lipperheide and H. Fiedeldey, Z. Phys. A **286**, 45 (1978); **301**, 81 (1981).

[5] H. Fiedeldey, R. Lipperheide, K. Naidoo, and S. A. Sofianos, Phys. Rev. C **30**, 434 (1984).

[6] L. J. Allen, K. Amos, C. Steward, and H. Fiedeldey, Phys. Rev. C **41**, 2021 (1990); L. J. Allen, H. Fiedeldey, S. A. Sofianos, K. Amos, and C. Steward, *ibid.* **44**, 1606 (1991); L. J. Allen, K. Amos, and H. Fiedeldey, J. Phys. G **18**, L179 (1992).

[7] D. R. Lun, X. J. Chen, L. J. Allen, and K. Amos, Phys. Rev. A **49**, 3788 (1994).
[8] L. J. Allen, Phys. Rev. A **34**, 2708 (1986); L. J. Allen and I. E. McCarthy, *ibid.* **36**, 2570 (1987); D. R. Lun, X. J. Chen, L. J. Allen, and K. Amos, *ibid.* **50**, 4025 (1994).
[9] T. Sakae, S. Sumiyoshi, F. Murakami, Y. Matsumoto, K. Ishibashi, and A. Katase, J. Phys. B **22**, 1385 (1989).
[10] W. H. Miller, J. Chem. Phys. **51**, 3631 (1969).
[11] R. Feltgen, H. Pauly, F. Torello, and H. Vehmeyer, Phys. Rev. Lett. **30**, 820 (1973).
[12] A. Zecca, G. Karwasz, R. S. Brusa, and C. Szmytkowski, J. Phys. B **24**, 2747 (1991).
[13] L. A. Collins and B. I. Schneider, in *Electron-Molecule Scattering and Photoionization,* edited by P. G. Burke and J. B. West (Plenum, New York, 1988), p. 147, and references cited therein.
[14] A. Jain, J. Chem. Phys. **81**, 724 (1984).
[15] P. A. Gianturco, A. Jain, and L. C. Pantano, J. Phys. B **20**, 571 (1987).
[16] A. Jain, Phys. Rev. A **34**, 3707 (1986).
[17] R. G. Newton, J. Math. Phys. **9**, 2050 (1968); R. B. Gerber and M. Karplus, Phys. Rev. D **1**, 998 ( 1970).
[18] A. Martin, Nuovo Cimento A **59**, 131 (1969).
[19] D. R. Lun, L. J. Allen, and K. Amos, Phys. Rev. A **50**, 4000 (1994).